Environment Protection Engineering

Vol. 36 2010 No. 4

ALICJA SIUTA-OLCHA*

ENERGY EFFICIENCY EVALUATION OF A SOLAR DOMESTIC HOT-WATER SYSTEM: A CASE STUDY

This paper presents the results of a simulation study of a solar domestic water heating system using the Exodus method. The simulations have been performed with three days of real weather data. Investigations of thermal conditions in the flat-plate solar collector–water-storage tank system enabled to carry out a detailed evaluation of energy efficiency of the solar installation. The influence of the flow rate of the medium in the collector cycle, of initial water temperature in the tank and of the solar irradiation for a day on the quantity of energy accumulated in this system was analyzed. The efficiency of energy accumulation in the tank at the stage of its loading and during hot-water consumption was determined.

1. INTRODUCTION

The application of heating systems with renewable energy sources has a positive impact on the natural environment limiting the air pollution [1]. The use of the solar hot-water heating systems is becoming more and more popular in Poland. In 2006, the total annual heat energy generated by all solar collectors installed in 48 countries of the world amounted to 76 959 GW·h. The consequence of the fact was the reduction of CO_2 emission by 34.1 million tonnes [2]. A typical solar water heating unit in the UK can reduce the domestic yearly hot-water load by up to 40%, representing 4.17 million tonnes of CO_2 per year in a national context or roughly 2.64% of the total CO_2 emissions [3]. There were 2.95 MW_{th} installed per 1 million inhabitants in Poland in 2006 [2]. Solar systems can operate effectively in the Polish climate conditions within the period of approximately 6–7 months, which means starting from the second decade of April to the third decade of October. The annual power output from 1 m^2 of collector absorber varies between 400 and 600 kW·h. In summertime, solar collectors should cover almost 100% demand for heat used for heating water to the temperature of 45 °C, in the quantity

* Faculty of Environmental Engineering, Lublin University of Technology, ul. Nadbystrzycka 40 B, 20-618 Lublin, Poland. E-mail: a.siuta-olcha@pollub.pl, tel.: 48-81 5384424, fax: 48-81 5381997.

corresponding to daily consumption. In a typical single-family house, 40–80 dm^3 of hot-water per one inhabitant is used daily, the water should be heated from 5–10 °C to the required temperature of 45–55 °C. Hot-water consumption in Danish single-family houses varies between 60 dm^3/day and 160 dm^3/day [4]. Artificial neural networks can be used for the modelling of time schedules of domestic hot-water consumption [5].

Energy effects attained by the solar system depend on: (i) geographical conditions, (ii) changeable climatic conditions, (iii) material-design parameters of the system elements, (iiii) operating conditions of the system. Thermal stratification in the storage tank increases the heat efficiency of the solar system [6]–[9]. In order to define the energy efficiency of solar systems, the dynamic simulation code TRNSYS is most frequently used [6], [10]. Numerical simulations have been carried out to investigate the influence of different levels of hot-water consumption on the thermal performance of small solar systems [7]. The results of simulation studies of the solar hot-water heating system consisting of a solar collector, a water-storage tank, an electric heater, and a water-mixing device using a time marching model were shown in [11]. Using a thermal model of finite differences, the influences of the flow rate and the stratification of the tank on the thermal performances of a solar system were analyzed in [12].

In this paper, simulation investigations of the thermal behaviour of a solar system consisting of a flat-plate solar collector and a water-storage tank with thermal stratification using the Exodus procedure were presented.

2. SOLAR WATER HEATING SYSTEM DESCRIPTION

The subject of the study was a small solar system used for preparation of hot-water in a single-family house occupied by four residents. The main components of the system are as follows: two solar collectors with a total surface of approximately 3.2 m^2, a storage tank with a capacity of 200 dm^3 as well as an electrical boiler with a capacity of 150 dm^3. Table 1 presents the technical parameters that characterize the solar collector–water-storage tank system. The operation of the solar installation was controlled by means of a step-by-step method with a circulation pump and a time regulator. The advantage of this method is that it is possible to maintain the water temperature gradient in the accumulation tank during the day and night, however, cooling of the storage tank on cloudy days can be a disadvantage. The solar system is provided with measuring equipment for continuous monitoring of its operation, including the pyranometer placed on the surface of the collectors, the sensor of outside air temperature and water meter equipped with a pulser. The average energy gain from solar collectors was defined at the level of 5513 MJ/year for the calculation conditions kept. The average annual rate of heat demand for heating hot-water which is covered by the solar system is therefore more than 50%. Figure 1 shows the percentage of heat demand for hot-water preparation foreseen to be covered by means of the solar system in particular months. The monthly average total solar radia-

tion on a tilted plane (60º) with the given orientation (SW) in W·h per square meter was assumed according to a meteorological database for the actinometric station in Warsaw. These data are available at http://www.mi.gov.pl.

Table 1

Data for the flat plate solar collector and hot water storage tank

Parameter	Description
Flat plate solar collector	
Dimensions: length×width×depth, mm	1920×830×95
Absorber area of collector, m^2	1.20
Glass cover thickness, mm	4
Absorber plate thickness, mm	3
Insulation thickness, mm	50
Flow channel diameter, mm	10
Collective fluid conduits diameter, mm	20
Absorber plate / flow channel material	steel/copper
Covering layers on absorbers	black galvanic chromium on a nickel-plated surface
Insulation material	polyurethane foam + Al film
Glass transmittance	0.80
Absorber plate absorptance	0.95
Maximum efficiency of the collector related to absorber surface	0.79
Collector tilt, °	60
Orientation	south-west
Water storage tank	
Tank material	steel
Volume, dm^3	200
Height/diameter, m	1.5/0.4
Insulation material	foamed polystyrene
Insulation thickness, mm	50

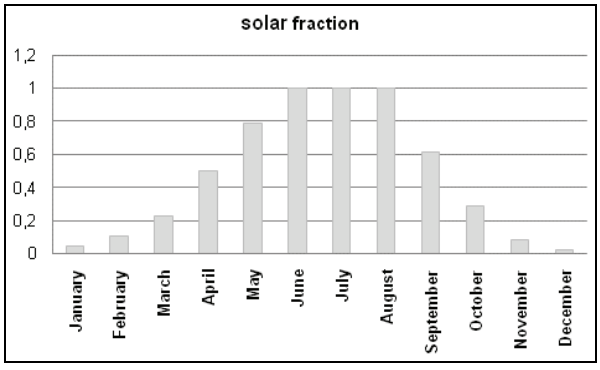

Fig. 1. The cover of heat demand for hot water preparation by the solar system in particular months

3. SIMULATION METHOD

Simulation investigations of thermal behaviour of the solar water heating system were conducted with using the following proprietary probabilistic models: the flat-plate solar collector for a non-steady state and the storage tank with thermal stratification. For the modelling of heat transfer processes in solar energy collector in non-steady conditions, the temporary energy balance for this i difference element in the stationary object can be expressed by the following formula:

$$V_i \rho_i c_{pi} \frac{dT_i}{d\tau} = \sum_j \dot{Q}_{ji} + \dot{Q}_{bi} + V_i \dot{q}_{vi} \,, \tag{1}$$

where: V_i – volume [m^3], ρ_i – density [kg/m^3], c_{pi} – fluid specific heat at constant pressure [J/(kg·K)], T_i – temperature of solar collector element with characteristic i node [K], τ – time [sec], $\dot{Q}_{ji}$ – thermal flux reaching i node from neighbouring j node [W], $\dot{Q}_{bi}$ – thermal flux reaching i node from boundary [W], $\dot{q}_{vi}$ – volumetric capacity of heat source [W/m^3].

In the thermal model of the solar collector, there were three isothermal nodes which were connected to the front cover, the absorber plate and the working medium. Temperatures in particular nodes are calculated from the following system of equations [13]:

$$\begin{cases} T_{g,\tau+1} = T_{g,\tau}\left[1 - \dfrac{\Delta\tau}{W_g}\left(\dfrac{1}{R_{gb}} + \dfrac{1}{R_{gp}}\right)\right] + \dfrac{\Delta\tau}{W_g}\left(\dfrac{T_{p,\tau}}{R_{gp}} + \dfrac{T_a}{R_{gb}} + P1_\tau\right), \\ T_{p,\tau+1} = T_{p,\tau}\left[1 - \dfrac{\Delta\tau}{W_p}\left(\dfrac{1}{R_{pb}} + \dfrac{1}{R_{pg}} + \dfrac{1}{R_{pf}}\right)\right] + \dfrac{\Delta\tau}{W_p}\left(\dfrac{T_{g,\tau}}{R_{pg}} + \dfrac{T_{f,\tau}}{R_{pf}} + \dfrac{T_a}{R_{pb}} + P2_\tau\right), \\ T_{f,\tau+1} = T_{f,\tau}\left[1 - \dfrac{\Delta\tau}{W_f}\left(\dfrac{1}{R_{fp}} + \dfrac{1}{R_f}\right)\right] + \dfrac{\Delta\tau}{W_f}\left(\dfrac{T_{p,\tau}}{R_{fp}} + \dfrac{T_{f,i}}{R_f}\right), \end{cases} \tag{2}$$

where: T_g – cover glass temperature [K], T_p – absorber plate temperature [K], T_f – outlet fluid temperature [K], $\Delta\tau$ – time interval = 1 sec, W_g – cover glass heat capacity [J/K], W_p – absorber plate heat capacity [J/K], W_f – fluid heat capacity [J/K], $P1$ – thermal energy emitted in glass cover in the middle of its thickness [W], $P2$ – thermal energy emitted on absorber plate surface [W], T_a – ambient temperature [K], R_{ij} – thermal resistance between differential element with i node and differential element with j node [K/W], R_f – thermal resistance of working fluid [K/W].

A detailed mathematical description of the thermal model of the solar collector making use of the Exodus procedure, as well as the solution of the equation of non-steady heat conduction in the solar collector were presented in [13].

The thermal model of the storage tank is composed of four sections. The temperatures of each of the i tank section are determined as follows:

- for $T_{f,\mathrm{col}} \geq T_1$

$$\begin{cases} T_{1,\tau+1} = T_{1,\tau}\left[1-\dfrac{\Delta\tau}{W_1}\left(\dfrac{1}{R_{1b}}+\dfrac{1}{R_{12}}+\dfrac{1}{R_{f,\mathrm{col}}}\right)\right]+T_{2,\tau}\dfrac{\Delta\tau}{W_1}\dfrac{1}{R_{12}}+T'_a\dfrac{\Delta\tau}{W_1}\dfrac{1}{R_{1b}} \\ \qquad +T_{f,\mathrm{col}\tau}\dfrac{\Delta\tau}{W_1}\dfrac{1}{R_{f,\mathrm{col}}}, \\ T_{2,\tau+1} = T_{2,\tau}\left[1-\dfrac{\Delta\tau}{W_2}\left(\dfrac{1}{R_{2b}}+\dfrac{1}{R_{21}}+\dfrac{1}{R_{23}}+\dfrac{1}{R_{f,2}}\right)\right]+T_{1,\tau}\left[\dfrac{\Delta\tau}{W_2}\left(\dfrac{1}{R_{21}}+\dfrac{1}{R_{f,2}}\right)\right] \\ \qquad +T_{3,\tau}\dfrac{\Delta\tau}{W_2}\dfrac{1}{R_{23}}+T'_a\dfrac{\Delta\tau}{W_2}\dfrac{1}{R_{2b}}, \\ T_{3,\tau+1} = T_{3,\tau}\left[1-\dfrac{\Delta\tau}{W_3}\left(\dfrac{1}{R_{3b}}+\dfrac{1}{R_{32}}+\dfrac{1}{R_{34}}+\dfrac{1}{R_{f,3}}\right)\right]+T_{2,\tau}\left[\dfrac{\Delta\tau}{W_3}\left(\dfrac{1}{R_{32}}+\dfrac{1}{R_{f,3}}\right)\right] \\ \qquad +T_{4,\tau}\dfrac{\Delta\tau}{W_3}\dfrac{1}{R_{34}}+T'_a\dfrac{\Delta\tau}{W_3}\dfrac{1}{R_{3b}}, \\ T_{4,\tau+1} = T_{4,\tau}\left[1-\dfrac{\Delta\tau}{W_4}\left(\dfrac{1}{R_{4b}}+\dfrac{1}{R_{43}}+\dfrac{1}{R_{f,4}}\right)\right]+T_{3,\tau}\left[\dfrac{\Delta\tau}{W_4}\left(\dfrac{1}{R_{43}}+\dfrac{1}{R_{f,4}}\right)\right] \\ \qquad +T'_a\dfrac{\Delta\tau}{W_4}\dfrac{1}{R_{4b}}, \end{cases} \tag{3}$$

- for $T_4 > T_L$

$$\begin{cases} T_{1,\tau+1} = T_{1,\tau}\left[1-\dfrac{\Delta\tau}{W_1}\left(\dfrac{1}{R_{1b}}+\dfrac{1}{R_{12}}+\dfrac{1}{R_{f,col}}\right)\right]+T_{2,\tau}\dfrac{\Delta\tau}{W_1}\dfrac{1}{R_{12}}+T'_a\dfrac{\Delta\tau}{W_1}\dfrac{1}{R_{1b}}, \\ T_{2,\tau+1} = T_{2,\tau}\left[1-\dfrac{\Delta\tau}{W_2}\left(\dfrac{1}{R_{2b}}+\dfrac{1}{R_{21}}+\dfrac{1}{R_{23}}+\dfrac{1}{R_{f,2}}\right)\right]+T_{1,\tau}\left[\dfrac{\Delta\tau}{W_2}\left(\dfrac{1}{R_{21}}+\dfrac{1}{R_{f,2}}\right)\right] \\ \qquad +T_{3,\tau}\dfrac{\Delta\tau}{W_2}\dfrac{1}{R_{23}}+T'_a\dfrac{\Delta\tau}{W_2}\dfrac{1}{R_{2b}}, \\ T_{3,\tau+1} = T_{3,\tau}\left[1-\dfrac{\Delta\tau}{W_3}\left(\dfrac{1}{R_{3b}}+\dfrac{1}{R_{32}}+\dfrac{1}{R_{34}}+\dfrac{1}{R_{f,3}}\right)\right]+T_{2,\tau}\left[\dfrac{\Delta\tau}{W_3}\left(\dfrac{1}{R_{32}}+\dfrac{1}{R_{f,3}}\right)\right] \\ \qquad +T_{4,\tau}\dfrac{\Delta\tau}{W_3}\dfrac{1}{R_{34}}+T'_a\dfrac{\Delta\tau}{W_3}\dfrac{1}{R_{3b}}, \\ T_{4,\tau+1} = T_{4,\tau}\left[1-\dfrac{\Delta\tau}{W_4}\left(\dfrac{1}{R_{4b}}+\dfrac{1}{R_{43}}+\dfrac{1}{R_{f,4}}\right)\right]+T_{3,\tau}\left[\dfrac{\Delta\tau}{W_4}\left(\dfrac{1}{R_{43}}+\dfrac{1}{R_{f,4}}\right)\right] \\ \qquad +T'_a\dfrac{\Delta\tau}{W_4}\dfrac{1}{R_{4b}}+T_L\dfrac{\Delta\tau}{W_4}\dfrac{1}{R_{f,L}}, \end{cases} \tag{4}$$

where: T_i – water temperature in i section [K], W_i – water heat capacity in i section [J/K], R_{ij} – thermal resistance between i section and j section [K/W], R_{ib} – thermal resistance between the storage tank and its surroundings for i section [K/W], $R_{f,i}$ – thermal resistance of water in i section, [K/W], $R_{f,\mathrm{col}}$ – thermal resistance of working fluid, [K/W], $R_{f,L}$ – thermal resistance of cold water, [K/W], $\Delta\tau$ – time interval = 1 sec, T'_a – ambient temperature for the tank [K], $T_{f,\mathrm{col}\,\tau}$ – outlet fluid temperature from the collector [K], T_L – temperature of cold water.

The Exodus procedure was applied in order to define thermal field in the tank and the detailed description of the application of this calculation method was presented in [14].

The Exodus procedure is one of the probabilistic methods for the approximate solution of heat transfer problems in real systems. What is characteristic of this procedure is a possibility of carrying out the heat exchange simulation with respect to the subject system considering changeable weather conditions and operating parameters of the solar system. This procedure enables relatively easy consideration of the variability of material parameters depending on temperature. It is specially recommended for the determination of temperature changes at one or several nodes of a geometrical network. Probabilistic methods enable us to determine the searched values with their specific maximum accuracy or probability allowing for non-linear thermal characteristics. The Exodus method can produce solutions to a class of thermal conduction problems faster than any conventional numerical method [13], [15].

Simulation calculations were conducted with CollSt.PAS software (the author of this program – Siuta-Olcha). Actual climate parameters (the total solar irradiance G, the ambient temperature T_a, the wind velocity v_w), averaged within one hour, and operating parameters (the volume flow rate of heat transfer fluid Q_{col}, the collector inlet fluid temperature T_{f1}, the volume flow rate of cold-water flowing in the tank) of the system were entered to the program. It was assumed that the temperature of water supplying the storage tank equals approximately the temperature of the medium flowing out of the collectors. Heat losses through the bottom and the upper part of the tank to the surroundings were not considered. The temperature gradient in radial direction was not considered either. The program for computer simulations was subject to verification based on experimental research the results of which were collated in [16]. Calculated temperatures in the distinguished nodes of the system constituted the basis for the evaluation of the energy efficiency of the hot-water solar system.

The daily mean efficiency is given by the following relation [6], [12]:

$$\eta_{\mathrm{day}} = \frac{\Sigma q_f}{A_c \int\limits_{\mathrm{sunrise}}^{\mathrm{sunset}} G(t)\mathrm{d}t}, \tag{5}$$

where: q_f – average useful energy gain [W], A_c – collectors area [m^2], G – total solar irradiance [W/m^2].

The solar collector efficiency can be obtained from:

$$\eta_c = \frac{\dot{m}_c c_p (T_{f2} - T_{f1})}{A_c G}, \tag{6}$$

where: $\dot{m}_c$ – circulated fluid mass-flow rate [kg/s], c_p – fluid specific heat [J/(kg·K)], T_{f1} – inlet fluid temperature [°C], T_{f2} – outlet fluid temperature [°C].

The energy accumulated in the system can be calculated on the basis of the formula:

$$E_p = m_{tn} c_p (T_{tn}^{\max} - T_{tn}^0), \tag{7}$$

where: m_{tn} – mass of water in the storage tank [kg], $T_{tn}^{\max}$ – maximum average water temperature in the storage tank [°C], T_{tn}^0 – initial water temperature inside the tank [°C].

The energy accumulation efficiency in the solar system for hot-water heating was described in the following way:

$$\eta = \frac{E_p}{A_c \sum_{i=1}^{n} G_i t_p}, \tag{8}$$

where t_p stands for time period [s].

4. RESULTS AND DISCUSSION

Simulation studies of the classical solar water heating installation, assuming its operation in actual conditions, were conducted for the three days of diversified weather conditions in June. The temperature around the storage tank was assumed to be equal to 18 °C, and the cold-water temperature amounted to 14 °C. The hot-water consumption resulting from residents' needs was taken into account. Figure 2 presents profiles of the daily domestic hot-water consumption.

Water heated in the solar collectors, supplying the storage tank, reached the highest temperature of 59 °C at 3 p.m. on June 19, 55.2 °C at 5 p.m. on June 21, 41.2 °C at 2 p.m. on June 25. Figures 3–5 illustrate distribution of water temperature in the storage tank for four distinguished levels on the assumption that there is no hot-water consumption. The tank was supplied with water, the temperature of which changed every hour, and with changeable volume flow rate in the solar collector cycle Q_{col}.

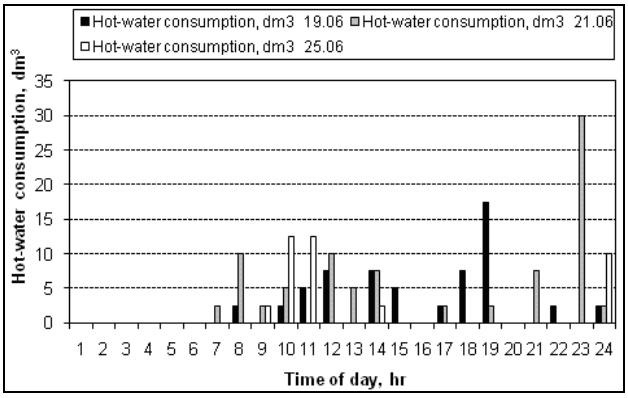

Fig. 2. Histograms of daily hot-water consumption for three distinguished days

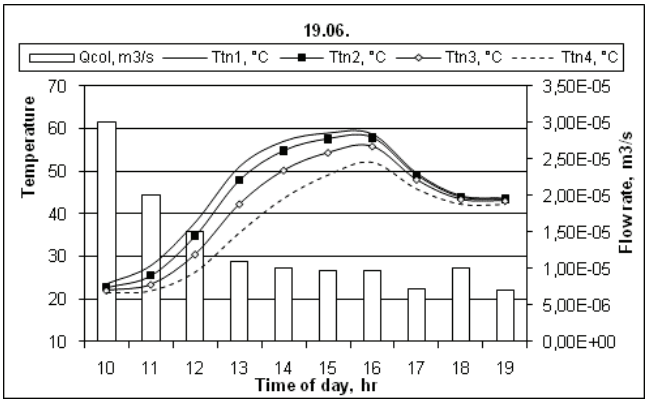

Fig. 3. Temperature distribution in the storage tank during charging (only) (Day 1)

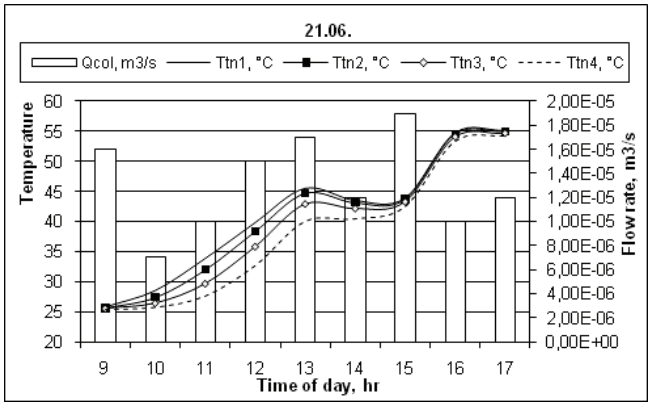

Fig. 4. Temperature distribution in the storage tank during charging (only) (Day 2)

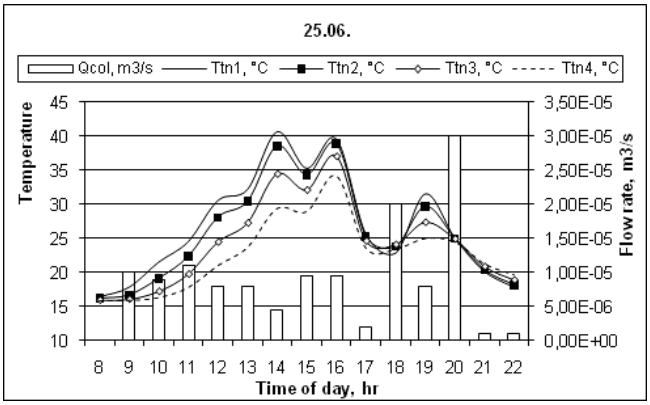

Fig. 5. Temperature distribution in the storage tank during charging (only) (Day 3)

On the first day the simulation was commenced at 10 a.m. assuming the following diversified water temperatures in the tank: T_{tn1} = 23.5 °C, T_{tn2} = 22.8 °C, T_{tn3} = 22 °C, T_{tn4} = 21.5 °C. The water temperature reached a maximum value at 4 p.m., for example, in the section No. 2 the temperature equalled 57.8 °C. The maximal degree of stratification ($T_{tn1} - T_{tn4}$) = 15.33 °C occurred at 1 p.m. Thermal water stratification in the tank disappears after 6 p.m. For the second day at the beginning of the simulation, equal temperature of water in the storage tank (25.5 °C) was assumed. Water in the tank reached the highest temperature of 55.1 °C at 5 p.m. The maximal degree of stratification ($T_{tn1} - T_{tn4}$) = 7 °C was observed at 12 p.m. In this case, equalization of water temperature in the tank occurred at about 3 p.m. The third day is characterized by adverse weather conditions. At 8 a.m. a slight change of water conditions in the tank was assumed: T_{tn1} = 16.4 °C, T_{tn2} = 16.2 °C, T_{tn3} = 15.9 °C, T_{tn4} = 15.8 °C. Water

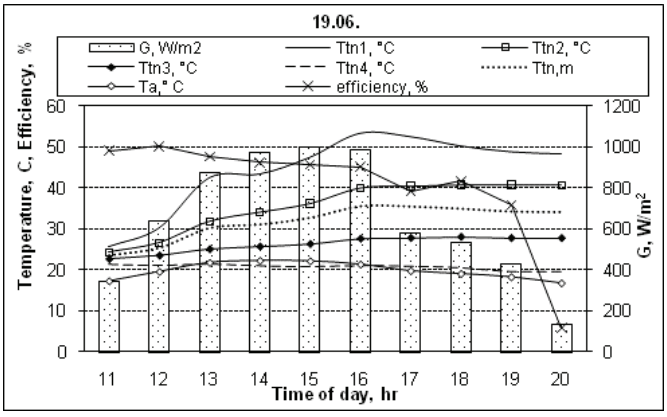

Fig. 6. Evolution of the collector's efficiency and storage fluid temperature for real conditions (Day 1): $T_{tn,m}$ – mean water temperature in the storage tank

in the tank was heated to the maximum temperature reaching 40.6 °C at 2 p.m., however, the average temperature in the tank attained the highest value (37.4 °C) at 4 p.m. The maximal stratification rate ($T_{tn1} - T_{tn4}$) = 11.2 °C appears at 2 p.m. A gradual stratification fading is observed after 4 p.m. Thereafter the thermal behaviours in the

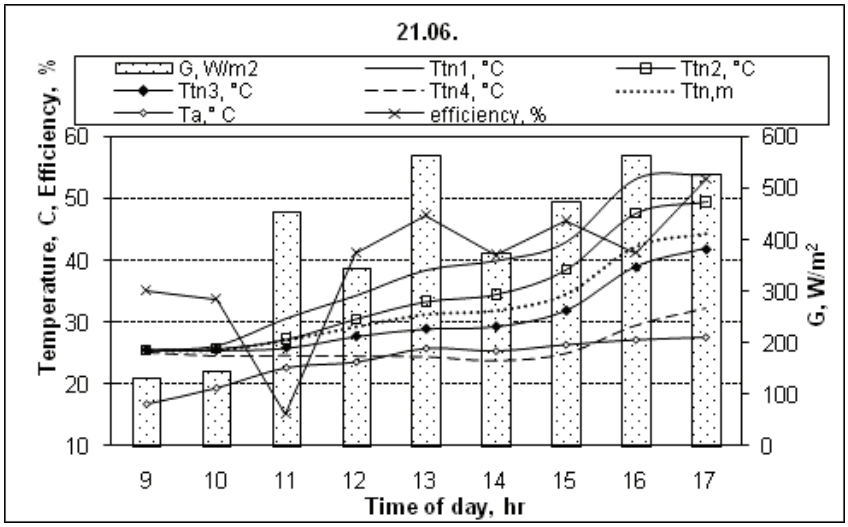

Fig. 7. Evolution of the collector's efficiency and storage fluid temperature for real conditions (Day 2): $T_{tn,m}$ – mean water temperature in the storage tank

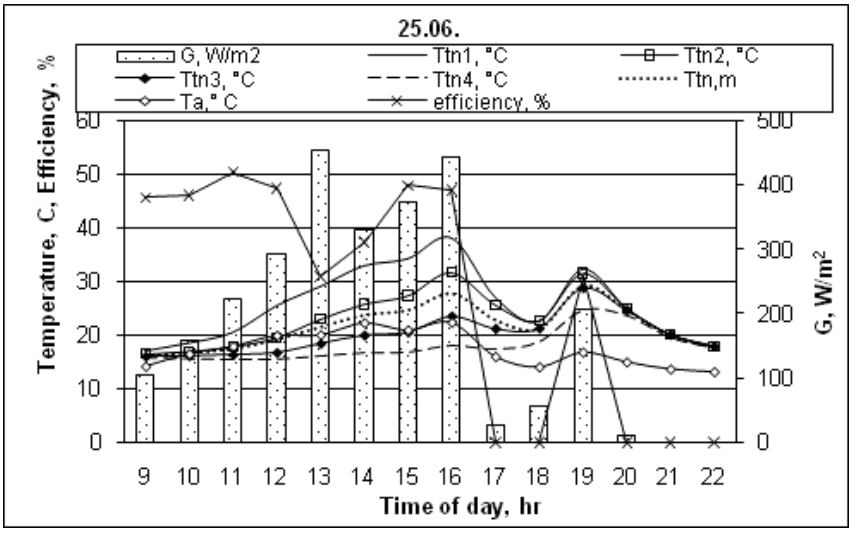

Fig. 8. Evolution of the collector's efficiency and storage fluid temperature for real conditions (Day 3): $T_{tn,m}$ – mean water temperature in the storage tank

solar collector–storage tank system, with consideration of some disturbances such as hot-water consumption, were analysed. Distributions of water temperature in the storage tank achieved on the basis of the simulation are presented in figures 6–8. Considering the first day (figure 6), the instantaneous efficiency of the solar collectors ranging from 35.8% to 50.1% between 11 a.m. and 7 p.m. was defined. Water in the tank attained the top temperature (53.3 °C) at 4 p.m., and the average water temperature was at the level of 35.4 °C. The maximal degree of stratification ($T_{tn1} - T_{tn4}$) = 32.2 °C was reported at 4 p.m. Thermal stratification in the storage tank was maintained during the whole day. As far as the second subject day (figure 7) is concerned, the efficiency of the solar collectors varied between 15.2% and 53.2% depending on daytime. The water temperature in the tank increased to 53.8 °C at 5 p.m. and the average water temperature was 44.3˚C. The maximal degree of stratification ($T_{tn1} - T_{tn4}$) = 23.6 °C was reported at 4 p.m. As regards the third case (figure 8), the efficiency of the solar collectors for particular hours ranged from 30.9% to 50.4%. Water in the top section was merely heated to the temperature of 38.1 °C at 4 p.m., and the average water temperature reached 29.3 °C at 7 p.m. The maximal stratification rate ($T_{tn1} - T_{tn4}$) = 20 °C was recorded at 4 p.m. The water temperature in the whole volume of the tank was equalized after 8 p.m. Figure 9 shows the influence of solar irradiation for a day on the efficiency and the amount of energy accumulated.

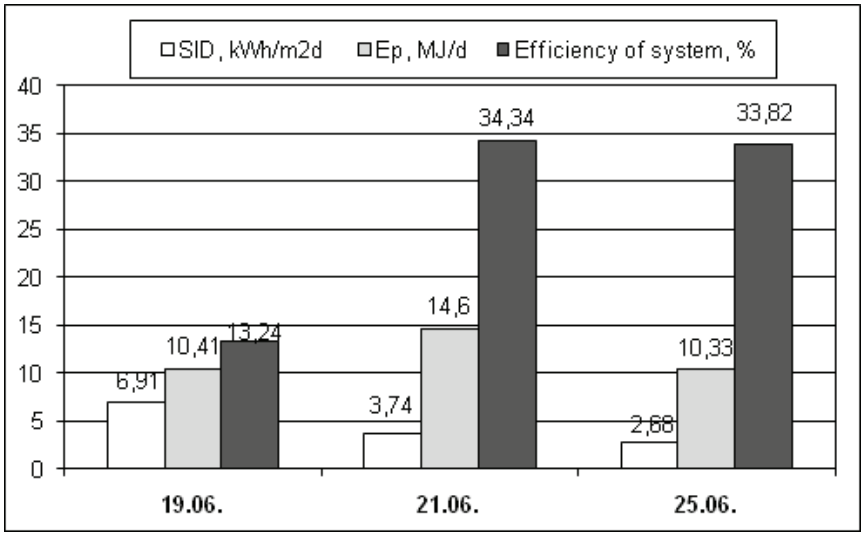

Fig. 9. Influence of a solar irradiation for a day (SID) on the efficiency and the energy accumulated in the solar system

Table 2 presents parameters characterizing the operation of the solar system.

Table 2

Characteristic parameters of the solar water heating system

Parameter	Day 1 (June 19)	Day 2 (June 21)	Day 3 (June 25)
Average daily hot-water consumption, dm^3/d	62.5	87.5	40
Average circulated fluid volume flow rate, m^3/s	$1.29 \cdot 10^{-5}$	$1.21 \cdot 10^{-5}$	$9.4 \cdot 10^{-6}$
Solar irradiation for a day (SID), $kW \cdot h/m^2 \cdot d$	6.91	3.74	2.68
Useful energy output of collectors, kW·h/d	228.36	110.24	82.1
Average efficiency of the solar collectors, %	41	39.4	27.4
Average storage of energy efficiency for charging the tank, %	34.2	54.4	55.4

5. CONCLUSIONS

The results of simulation calculations let us conclude that the heat removal from the tank during an active acquisition of the solar energy increases the thermal efficiency of solar collectors. A solar irradiation for a day does not have any influence on energy accumulation efficiency in the solar water heating system, however, the bigger the daily insulation dose, the higher the temperature at the outlet of the collector and more usable energy is attainable from the solar radiation conversion in the flat-plate solar collectors. The temperature rise in the tank is dependent on the intensity of the solar radiation. The lower the flow rate of the medium in the collector cycle, the higher the accumulation efficiency.

ACKNOWLEDGEMENTS

This work was supported by the Ministry of Science and Higher Education, Grant No. N N523 4136 35.

REFERENCES

[1] ZIMNY J., MICHALAK P., *The work of a heating system with renewable energy sources (RES) in school building*, Environment Protection Engineering, 2008, Vol. 34, No. 1, 81–88.
[2] CHWIEDUK D., *Rozwój słonecznej energetyki cieplnej*, Czysta Energia, 2009, 3, 16–18.
[3] MONDOL J.D., SMYTH M., ZACHAROPOULOS A., HYDE T., *Experimental performance evaluation of a novel heat exchanger for a solar hot water storage system*, Applied Energy, 2009, Vol. 86, No. 9, 1492–1505.
[4] FURBO S., ANDERSEN E., KNUDSEN S., VEJEN N.K., SHAH L. J., *Smart solar tanks for small solar domestic hot water systems*, Solar Energy, 2005, Vol. 78, No. 2, 269–279.
[5] CIEŻAK W., SIWOŃ Z., CIEŻAK J., *Modelowanie poboru wody w osiedlach mieszkaniowych*, Ochrona Środowiska, 2008, Vol. 30, No. 2, 23–28.
[6] DUFFIE J.A., BECKMAN W.A., *Solar Engineering of Thermal Processes*, John Wiley & Sons, Inc, Hoboken, New Jersey, 2006.
[7] KNUDSEN S., *Consumer's influence on the thermal performance of small SDHW systems – theoretical investigations*, Solar Energy, 2002, Vol. 73, No. 1, 33–42.
[8] ZACHAR A., FARKAS I., SZLIVKA F., *Numerical analyses of the impact of plates for thermal stratification inside a storage tank with upper and lower inlet flows*, Solar Energy, 2003, Vol. 74, No. 4, 287–302.

[9] GARNIER C., CURRIE J., MUNEER T., *Integrated collector storage solar water heater: Temperature stratification*, Applied Energy, 2009, Vol. 86, No. 9, 1465–1469.
[10] CARDINALE N., PICCININNI F., STEFANIZZI P., *Economic optimization of low-flow solar domestic hot water plants*, Renewable Energy, 2003, Vol. 28, No. 12, 1899–1914.
[11] BOJIĆ M., KALOGIROU S., PETRONIJEVIĆ K., *Simulation of a solar domestic water heating system using a time marching model*, Renewable Energy, 2002, Vol. 27, No. 3, 441–452.
[12] CRISTOFARI C., NOTTON G., POGGI P., LOUCHE A., *Modelling and performance of a copolymer solar water heating collector*, Solar Energy, 2002, Vol. 72, No. 2, 99–112.
[13] SIUTA-OLCHA A., *Application of a probabilistic method for determination of the thermal field in a flat-plate solar collector*, Archives of Environmental Protection, 2007, Vol. 33, No. 4, 67–81.
[14] SIUTA-OLCHA A., *Badania modelu wodnego zbiornika akumulacyjnego metodą Exodus*, [in:] *Techniczne, ekologiczne i ekonomiczne aspekty energetyki odnawialnej*, edited by CHOCHOWSKI A., Wydawnictwo SGGW, Warszawa, 2001, 112–122.
[15] MINKOWYCZ W.J., SPARROW E.M., MURTHY J.Y. *Handbook of Numerical Heat Transfer*, John Wiley & Sons, Inc, Hoboken, New Jersey, 2006.
[16] SIUTA-OLCHA A., *Thermal processes in solar domestic hot-water system*, Environment Protection Engineering, 2006, Vol. 32, No. 1, 95–101.